Volume 217, Issue 6, 15 November 2010 ISSN 0096-3003

APPLIED MATHEMATICS AND COMPUTATION

Applied Mathematics and Computation 217 (2010) 2773–2787

Contents lists available at ScienceDirect

Applied Mathematics and Computation

journal homepage: www.elsevier.com/locate/amc

The Singular Function Boundary Integral Method for singular Laplacian problems over circular sections

Evgenia Christodoulou, Christos Xenophontos, Georgios C. Georgiou *

Department of Mathematics and Statistics, University of Cyprus, P.O. Box 20537, 1678 Nicosia, Cyprus

ARTICLE INFO

Keywords:
Boundary singularities
Boundary approximation methods
Lagrange multipliers
Stress intensity factors

ABSTRACT

The Singular Function Boundary Integral Method (SFBIM) for solving two-dimensional elliptic problems with boundary singularities is revisited. In this method the solution is approximated by the leading terms of the asymptotic expansion of the local solution, which are also used to weight the governing partial differential equation. The singular coefficients, i.e., the coefficients of the local asymptotic expansion, are thus primary unknowns. By means of the divergence theorem, the discretized equations are reduced to boundary integrals and integration is needed only far from the singularity. The Dirichlet boundary conditions are then weakly enforced by means of Lagrange multipliers, the discrete values of which are additional unknowns. In the case of two-dimensional Laplacian problems, the SFBIM converges exponentially with respect to the numbers of singular functions and Lagrange multipliers. In the present work the method is applied to Laplacian test problems over circular sectors, the analytical solution of which is known. The convergence of the method is studied for various values of the order p of the polynomial approximation of the Lagrange multipliers (i.e., constant, linear, quadratic, and cubic), and the exact approximation errors are calculated. These are compared to the theoretical results provided in the literature and their agreement is demonstrated.

1. Introduction

In the last few decades there has been an extensive study of planar elliptic boundary value problems with boundary singularities. The methods that have been proposed for the solution of such problems range from special mesh-refinement schemes to sophisticated techniques that incorporate, directly or indirectly, the form of the local asymptotic expansion, which is known in many occasions. These methods aim to improve the accuracy and resolve the convergence difficulties that are known to appear in the neighborhood of singular points.

The local solution, centered at the singular point, in polar coordinates (r, θ) is of the general form

$$u(r,\theta) = \sum_{j=1}^{\infty} \alpha_j r^{\mu_j} f_j(\theta), \qquad (1)$$

where μ_j, f_j are, respectively, the eigenvalues and eigenfunctions of the problem, which are uniquely determined by the geometry and the boundary conditions along the boundaries sharing the singular point. The singular coefficients α_j also known as generalized stress intensity factors [1] or flux intensity factors [2], are determined by the boundary conditions in the rest of the boundary. Knowledge of the singular coefficients is of importance in many engineering applications, especially in fracture mechanics.

* Corresponding author.
E-mail address: georgios@ucy.ac.cy (G.C. Georgiou).

0096-3003/$ - see front matter © 2010 Elsevier Inc. All rights reserved.
doi:10.1016/j.amc.2010.08.012

In the past few years, Georgiou and co-workers [3–6] developed the Singular Function Boundary Integral Method (SFBIM), in which the unknown singular coefficients are calculated directly. The solution is approximated by the leading terms of the local asymptotic solution expansion and the Dirichlet boundary conditions are weakly enforced by means of Lagrange multipliers. The method has been tested on standard Laplacian and biharmonic problems, yielding extremely accurate estimates for the leading singular coefficients, and exhibiting exponential convergence with respect to the number of singular functions. Theoretical results on the convergence of the method in the case of Laplacian problems where given by Xenophontos et al. in [5].

The SFBIM belongs to the class of boundary approximation methods (BAMs) or Trefftz methods (TM), which have been recently reviewed by Li and co-workers [7] and compared to collocation and other boundary methods. Other recent reviews of methods used for elliptic boundary value problems with boundary singularities can be found in the articles of Bernal et al. [8] who considered both global and local meshless collocation methods with multiquadrics as basis functions, and of Dosiyev and Buranay [9] who employed the block method which was proposed for the solution of Laplace problems on arbitrary polygons.

The objective of this work is to apply the SFBIM to two model Laplacian problems over circular sections in order to investigate the effect of the order of the Lagrange multiplier approximation in connection with the theoretical error estimates.

In Section 2, two general plane Laplacian problems over circular sections are presented. One problem has Dirichlet and the other Neumann boundary conditions along the arc. The formulation of the method for both cases is given in Section 3. In Section 4, results are presented for piecewise constant, linear, quadratic and cubic basis functions, used for the approximation of the Lagrange multipliers. These results are compared with the theoretical error estimates. Finally, Section 5 summarizes the conclusions.

2. Test problems

We consider two Laplacian test problems over circular sectors of angle $\alpha\pi$ and radius R as depicted in Fig. 1. A boundary singularity occurs at the origin which is due, not only to the geometry (i.e., the presence of an angle in the boundary) but also to the fact that different boundary conditions are imposed on the boundary parts S_1 ($\theta = 0$) and S_2 ($\theta = \alpha\pi$). The two test problems differ only in the boundary condition along the circular arc S_3, where Dirichlet and Neumann boundary conditions are respectively prescribed. For both problems the local solution is

$$u = \sum_{j=1}^{\infty} \alpha_j r^{\mu_j} \sin(\mu_j \theta). \tag{2}$$

In problem 1 (Fig. 1(a)), the Dirichlet boundary condition along S_3 is given by

$$u = f(\theta) = \theta - \frac{\theta^2}{2\alpha\pi}. \tag{3}$$

In problem 2 (Fig. 1(b)), the Neumann boundary condition along S_3 is given by

$$\frac{\partial u}{\partial r} = g(\theta) = \frac{\theta}{\alpha\pi}. \tag{4}$$

For both problems, we have

$$\mu_j = \frac{2j-1}{2\alpha}. \tag{5}$$

The singular coefficients for problem 1 are given by

$$\alpha_j = \frac{16\alpha}{\pi^2 R^{\mu_j} (2j-1)^3} \tag{6}$$

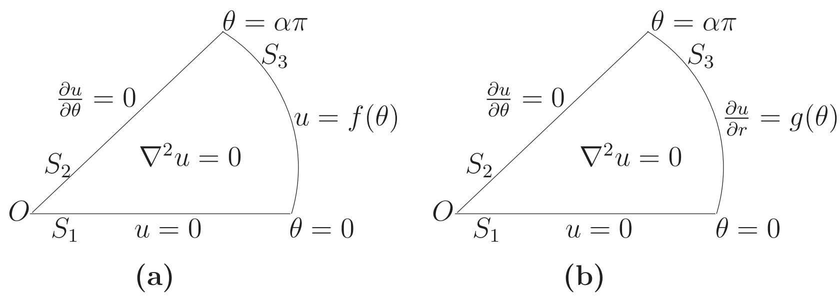

Fig. 1. Test Laplacian problems over circular sectors. (a) Problem 1 (b) Problem 2.

and for problem 2 by

$$\alpha_j = \frac{(-1)^{j+1}16\alpha}{\pi^2 R^{\mu_j - 1}(2j-1)^3}. \tag{7}$$

3. Formulation of the SFBIM

The SFBIM is based on the approximation of the solution by the leading terms of the local solution expansion:

$$u_N = \sum_{j=1}^{N_\alpha} \alpha_j^N W_j, \tag{8}$$

where N_α is the number of singular functions $W_j = r^{\mu_j}\sin(\mu_j\theta)$. Note that this approximation is valid only if the domain of the problem, Ω, is a subset of the convergence domain of expansion (2). By applying Galerkin's principle, the problem is discretized as follows:

$$\int\int_\Omega W_j \nabla^2 u_N \, dV = 0, \quad j = 1, 2, \ldots, N_\alpha. \tag{9}$$

By double application of Green's second identity, and keeping in mind that the singular functions W_j are harmonic, the above volume integral becomes

$$\int_{\partial\Omega} W_j \frac{\partial u_N}{\partial n} \, dS - \int_{\partial\Omega} u_N \frac{\partial W_j}{\partial n} \, dS = 0, \quad j = 1, 2, \ldots, N_\alpha. \tag{10}$$

This reduces the dimension of the problem by one and leads to considerable reduction in the computational cost. Now, since the W_j's satisfy the boundary conditions along S_1 and S_2, the above integral along these boundaries is zero. Therefore, we get

$$\int_{S_3} \left(W_j \frac{\partial u_N}{\partial n} - u_N \frac{\partial W_j}{\partial n} \right) dS = 0, \quad j = 1, 2, \ldots, N_\alpha. \tag{11}$$

It should be noted that integration is needed only along S_3, i.e., far from the singularity and not along the boundary parts causing the singularity.

3.1. Formulation of problem 1

The Dirichlet condition along S_3 is imposed by means of a Lagrange multiplier function λ, which replaces the normal derivative. The function λ is expanded in terms of standard polynomial basis functions M_i of order p:

$$\lambda = \frac{\partial u_N}{\partial n} = \sum_{i=1}^{N_\lambda} \lambda_i M_i, \tag{12}$$

where N_λ represents the total number of unknown discrete Lagrange multipliers λ_i (or, equivalently, the total number of Lagrange multiplier nodes) along S_3. The basis functions M_i are used to weigh the Dirichlet condition along the corresponding boundary segment S_3. Hence, we obtain the following symmetric system of $N_\alpha + N_\lambda$ discretized equations:

$$\int_{S_3} \left(\lambda W_j - u_N \frac{\partial W_j}{\partial n} \right) dS = 0, \quad j = 1, 2, \ldots, N_\alpha, \tag{13}$$

$$\int_{S_3} u_N M_i \, dS = \int_{S_3} f(r,\theta) M_i \, dS, \quad i = 1, 2, \ldots, N_\lambda. \tag{14}$$

The above system can be written in (block) matrix form as

$$\begin{bmatrix} D_{N_\alpha \times N_\alpha} & K_{N_\alpha \times N_\lambda} \\ K^T_{N_\lambda \times N_\alpha} & O_{N_\lambda \times N_\lambda} \end{bmatrix} \begin{bmatrix} A \\ \Lambda \end{bmatrix} = \begin{bmatrix} O \\ F \end{bmatrix}, \tag{15}$$

where A and Λ are, respectively, the vectors of unknown singular coefficients and Lagrange multipliers. It turns out that for this simple geometry the submatrix D is always diagonal with

$$D_{ii} = -\mu_i R^{2\mu_i} \frac{\alpha\pi}{2}. \tag{16}$$

The submatrix K and the forcing vector F are given by

$$K_{ij} = R^{\mu_i + 1} \int_0^{\alpha\pi} M_j \sin \mu_i\theta \, d\theta, \tag{17}$$

$$F_i = R \int_0^{\alpha\pi} f(\theta) M_i \, d\theta, \tag{18}$$

and can be calculated analytically for various orders p of the approximation of the Lagrange multiplier function. The entries in K and F for $p = 0, 1, 2$ and 3 are given in Appendix A.

According to the analysis in [5], if $\lambda \in H^k(S_3)$ for some $k \geqslant 1$ and λ_h is the approximation to the Lagrange multiplier function with h being the meshwidth, then there exist positive constants C and $\beta \in (0,1)$, independent of N_α and h such that

$$\|u - u_N\|_{1,\Omega} + \|\lambda - \lambda_h\|_{-1/2,S_3} \leqslant C\left\{\sqrt{N_\alpha}\beta^{N_\alpha} + h^m p^{-k}\right\}, \tag{19}$$

where $m = \min\{k, p+1\}$. Here, $H^k(\Omega), k \in \mathbb{N}$ is the usual Sobolev space which contains functions that have k generalized derivatives in the space of squared integrable functions $L^2(\Omega)$. The norm $\|\cdot\|_{1,\Omega}$ is defined, as usual, by

$$\|f\|_{1,\Omega} := \left[\int_\Omega \left\{f^2 + f_x^2 + f_y^2\right\} dx\,dy\right]^{1/2}. \tag{20}$$

The norm $\|\cdot\|_{-1/2,S_3}$ that appears in (19) is defined as follows: Let $H^{1/2}(S_3)$ denote the space of functions in $H^1(\Omega)$ whose (trace) values on S_3 belong to $L^2(S_3)$, let $T : H^1(\Omega) \to H^{1/2}(S_3)$ denote the trace operator, and define the norm

$$\|\psi\|_{1/2,S_3} = \inf_{u \in H^1(\Omega)} \left\{\|u\|_{1,\Omega} : Tu = \psi\right\}. \tag{21}$$

Then,

$$\|\phi\|_{-1/2,S_3} = \sup_{\psi \in H^{1/2}(S_3)} \frac{\int_{S_3} \phi\psi}{\|\psi\|_{1/2,S_3}}. \tag{22}$$

For more details see [5].

From (19) it is clear that the approximate solution converges exponentially with respect to the number of singular functions, N_α. Moreover, if we choose the two errors in (19) to be balanced, we obtain the following relationship between the number of singular functions and the number of basis functions used to approximate the Lagrange multiplier:

$$h^p \approx \sqrt{N_\alpha}\beta^{N_\alpha} \iff \left(\frac{\alpha\pi}{N_\lambda - 1}\right)^p \approx \sqrt{N_\alpha}\beta^{N_\alpha} \Rightarrow N_\lambda \approx 1 + \frac{\alpha\pi}{\left(\sqrt{N_\alpha}\beta^{N_\alpha}\right)^{1/p}}. \tag{23}$$

It was also shown in [5] that

$$|\alpha_j - \alpha_j^N| \leqslant C\beta^{N_\alpha}, \tag{24}$$

which shows that the approximate singular coefficients α_j^N converge exponentially with respect to the number of singular functions.

3.2. Formulation of problem 2

To impose the Neumann conditions, the normal derivative in (11) is simply substituted by the known function g. It turns out that for this problem all integrations can be performed analytically as this substitution gives

$$\int_{S_3} u_N \frac{\partial W_i}{\partial n}\, dS = \int_{S_3} g W_i\, dS, \quad i = 1, 2, \ldots, N_\alpha. \tag{25}$$

The above expression becomes

$$\alpha_i R^{2\mu_i - 1} \mu_i \int_0^{\alpha\pi} \sin^2(\mu_i\theta) d\theta = R^{\mu_i} \int_0^{\alpha\pi} g(\theta) \sin(\mu_i\theta) d\theta, \tag{26}$$

from which we find that

$$\alpha_i = \frac{4}{R^{\mu_i - 1}\pi(2i-1)} \int_0^{\alpha\pi} g(\theta)\sin(\mu_i\theta) d\theta = \frac{(-1)^{i+1} 16\alpha}{R^{\mu_i - 1}\pi^2(2i-1)^3}, \tag{27}$$

and the method is equivalent to the method of separation of variables. In the next section we will present numerical results for the first test problem.

4. Numerical results

Here we present the results of numerical computations in order to verify the theoretical results from [5].

4.1. Semi-circle ($\alpha = 1$)

First we consider the case $\alpha = 1$ for the angle θ, which corresponds to the domain being a semi-circle. Our first step was to determine the constant β appearing in (19), which was done as follows: We choose a value for N_λ, say $N_\lambda = 10$, and solve the linear system (11) for various values of $N_\alpha > 10$, using, e.g., $p = 2$. Concentrating on the first singular coefficient, we record the results in Table 1. Since the exact value of the first coefficient is $\alpha_1 = 16/\pi^2 \approx 1.621138938277404$, we see from the results of Table 1 that α_1^N has "converged" once $N_\alpha = 30$. Hence, using (23) and the "optimal" pair $N_\alpha = 30$, $N_\lambda = 10$ we compute the value for β as $\beta \approx 0.88$.

With β known, we use (24) to determine subsequent "optimal" values for N_λ and N_α, for use in our computations. We should note that in general, the exact value of the first coefficient is unknown, hence in practice we choose the "optimal" value of N_α based on the changes that appear in the computed α_1^N, i.e., once the value of α_1^N does not change significantly.

In Fig. 2 we show the convergence of the approximate solution and in particular the percentage relative error in the approximation of u versus N_α, in a semi-log scale for $p = 1, 2, 3$. Since each curve becomes a straight line as N_α is increased, we see that the error decreases at an exponential rate and the convergence as predicted by (19) is verified.

Figs. 3–5 show the percentage relative error in the first four singular coefficients, versus N_α in a semi-log scale, for $p = 1, 2, 3$, respectively. The exponential convergence as predicted by (24) is again readily visible in all three plots.

Next, we would like to compute the error in the approximation of the Lagrange multipliers. Note that for any $v \in H^{-1/2}(S_3)$ we have

$$\|v\|_{-1/2,S_3} \leqslant C\|v\|_{0,S_3} \leqslant \widehat{C}\|v\|_{\infty,S_3}, \quad C, \widehat{C} \in \mathbb{R}. \tag{28}$$

So, instead of $\|\lambda - \lambda_h\|_{-1/2,S_3}$, we use

$$100 \times \max_k \frac{|\lambda(\theta_k) - \lambda_h(\theta_k)|}{|\lambda(\theta_k)|} \tag{29}$$

where θ_k are the (internal) nodal points along S_3. By construction, $\lambda_h(\theta_k) = \lambda_k$, i.e., $\lambda_h(\theta_k)$ is equal to the kth discrete Lagrange multiplier. Fig. 6 shows this error versus N_λ (which is directly related to the meshwidth h on S_3) in a log–log scale. The convergence rate indeed appears to be algebraic of order p, i.e., $\lambda_h \to \lambda$ as $N_\lambda \to \infty$ (or, equivalently, as $h \to 0$) at the rate $O(N_\lambda^{-p})$ (or $O(h^p)$). Therefore, from (28) we have that $\|\lambda - \lambda_h\|_{-1/2,S_3} = O(h^p)$.

Finally, we show numerical results for the case $p = 0$. The error analysis in [5] does not cover this case, hence it is not possible to use (24) to determine "optimal" values for N_λ and N_α. In what follows we have chosen $N_\alpha = 2N_\lambda$; other choices gave similar results. Fig. 7 shows the percentage relative error in the first four singular coefficients versus N_α in a log–log scale. We observe that for $p = 0$, the convergence is not exponential, but rather algebraic of order 3.

Fig. 8 shows the percentage relative error in the approximation of u and of the Lagrange multipliers, versus N_α in a log–log scale. Again we have algebraic convergence, with rate 2 for the approximation of u and with rate 3/4 for the approximation of the Lagrange multipliers.

Table 1
Approximate singular coefficient a_1^N, computed with $N_\lambda = 10$, $\alpha = 1$.

N_α	α_1^N
12	1.617187500000000
13	1.621215820312500
14	1.619140625000000
15	1.621154785156250
16	1.622070312500000
17	1.621398925781250
18	1.621582031250000
19	1.621154785156250
20	1.621215820312500
21	1.621138935554673
22	1.621138937140710
23	1.621138937635686
24	1.621138937869855
25	1.621138938004718
26	1.621138938092001
27	1.621138938152942
28	1.621138938197758
29	1.621138938231953
30	**1.621138938258757**
31	1.621138938280287
32	1.621138938297822
33	1.621138938312330
34	1.621138938324523
35	1.621138938334964
36	1.621138938344132
37	1.621138938352468
38	1.621138938360383
39	1.621138938368192
40	1.621138938368413

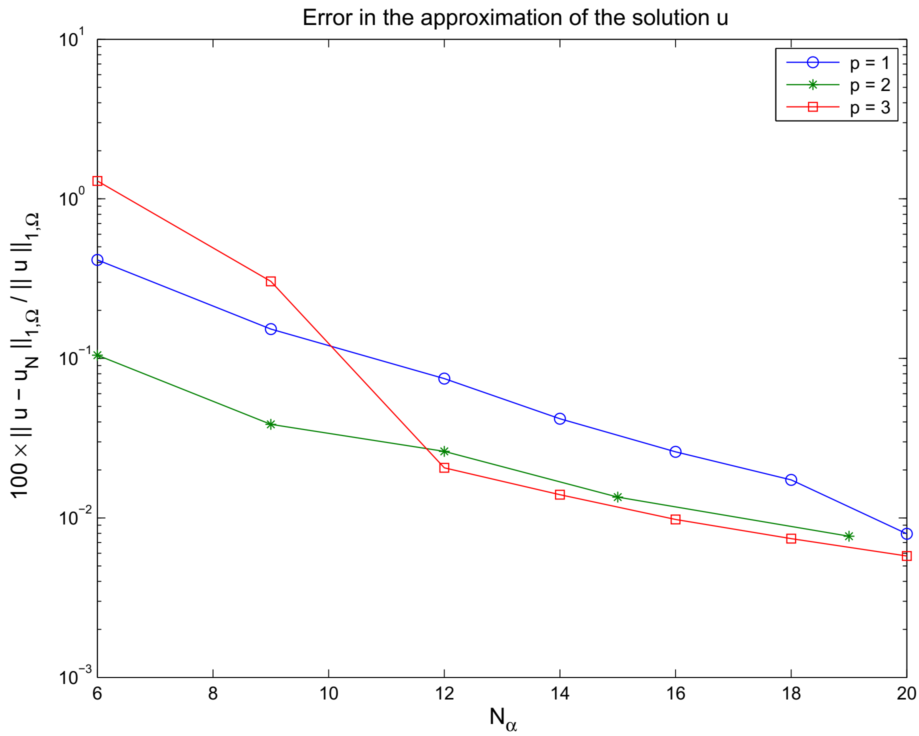

Fig. 2. Convergence of the approximate solution u_N, $\alpha = 1$.

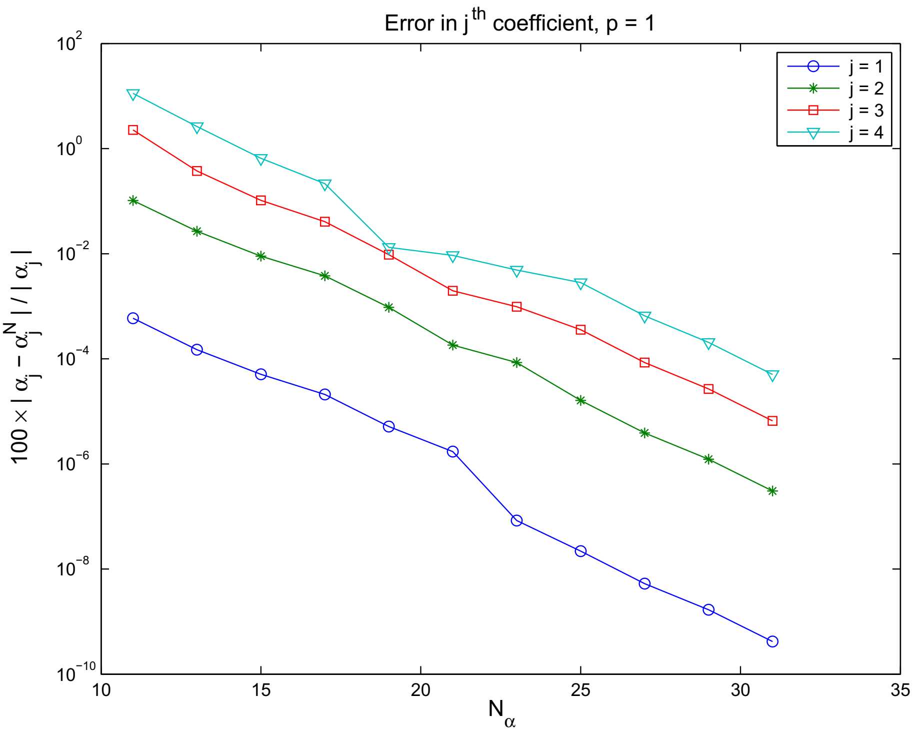

Fig. 3. Convergence of the singular coefficients α_j^N for $p = 1$, $\alpha = 1$.

4.2. Domain with a "slit" ($\alpha = 2$)

We have also repeated the previous computations for the case of $\alpha = 2$, which corresponds to a domain with a "slit". The procedure for determining the constant β in (19) was repeated yielding $\beta = 0.92$ for the pair $N_\alpha = 35$ and $N_\lambda = 20$.

Fig. 9 shows the convergence of the approximate solution and in particular the percentage relative error in the approximation of u versus N_α, in a semi-log scale for $p = 1, 2, 3$. As with α=1, each curve becomes a straight line as N_α is increased, hence the error decreases at an exponential rate as predicted by (19).

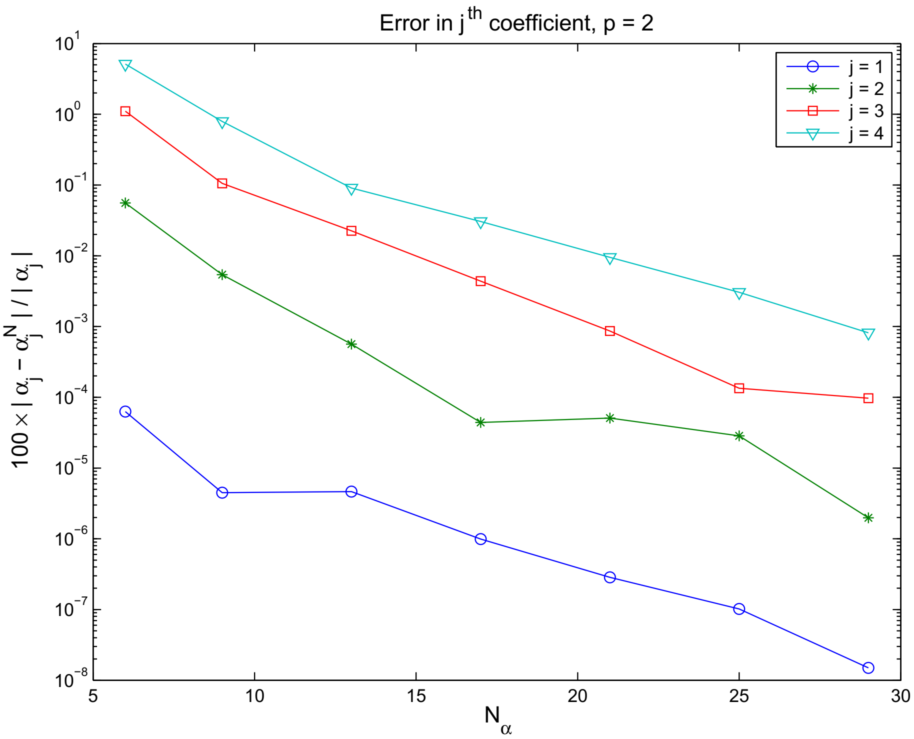

Fig. 4. Convergence of the singular coefficients α_j^N for $p = 2$, $\alpha = 1$.

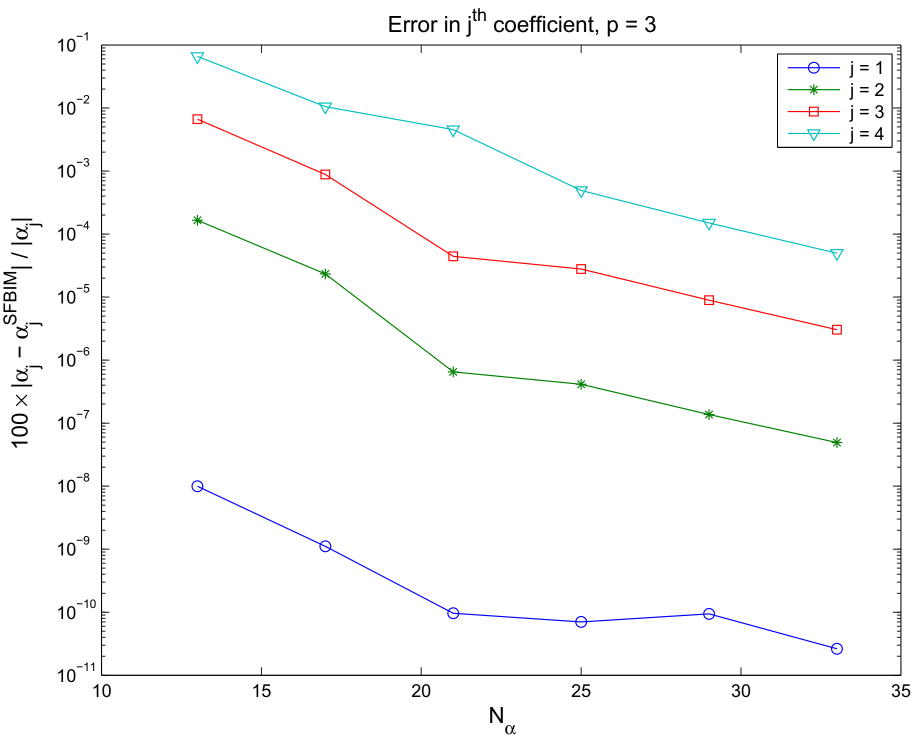

Fig. 5. Convergence of the singular coefficients α_j^N for $p = 3$, $\alpha = 1$.

Figs. 10 and 11 show the percentage relative error in the first four singular coefficients, versus N_α in a semi-log scale, for $p = 1$ and 2, respectively (the case $p = 3$ is almost identical). The exponential convergence is again visible in both plots.

Finally, Fig. 12 shows the error in the Lagrange multipliers versus N_λ in a log–log scale. The convergence rate again appears to be algebraic of order p.

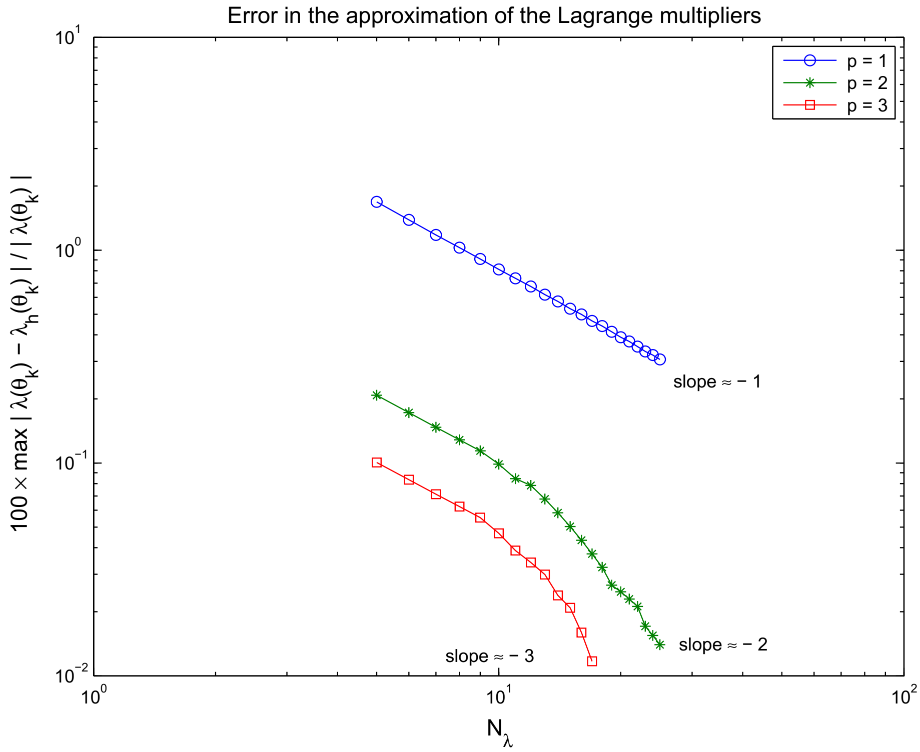

Fig. 6. Convergence of the Lagrange multipliers, $\alpha = 1$.

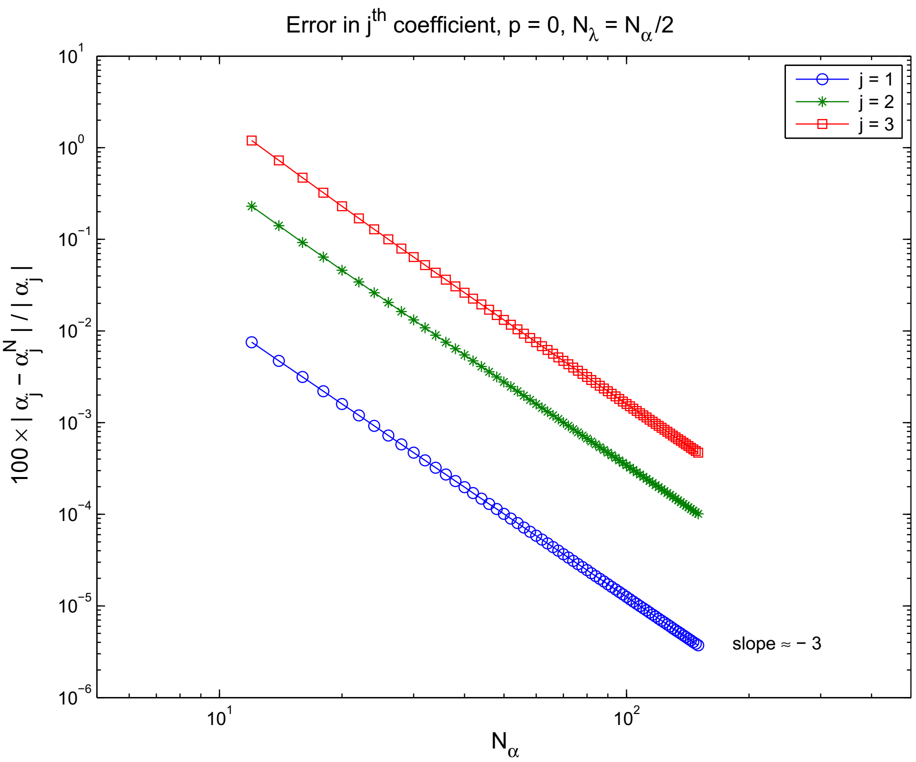

Fig. 7. Convergence of the singular coefficients α_j^N for $p = 0$, $\alpha = 1$.

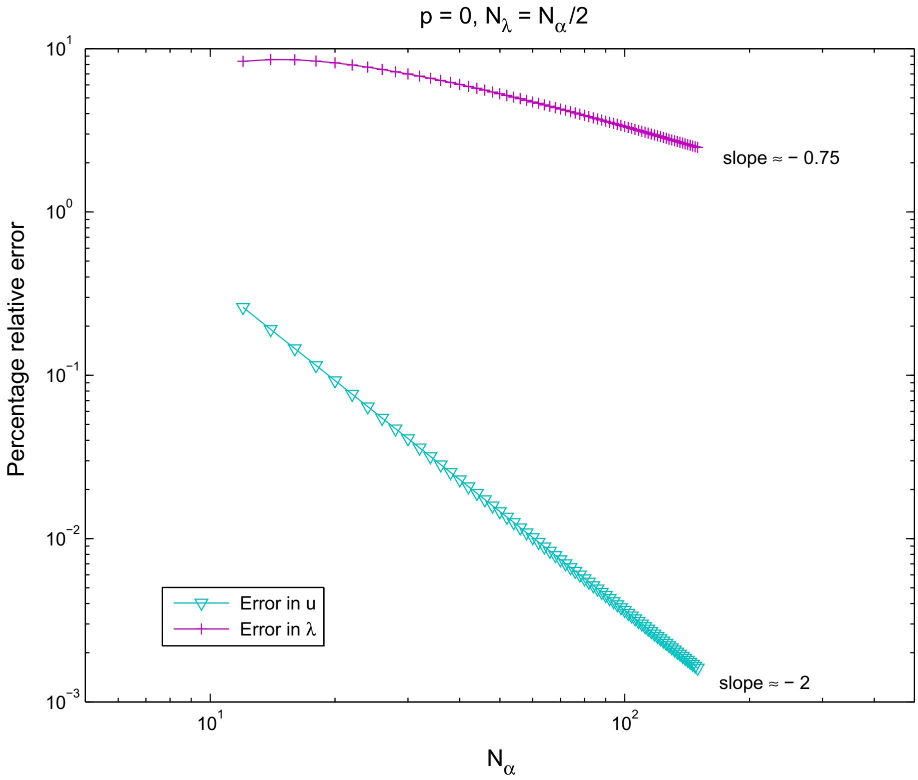

Fig. 8. Convergence of the approximate solution u_N and Lagrange multiplier λ_h for $p = 0$, $\alpha = 1$.

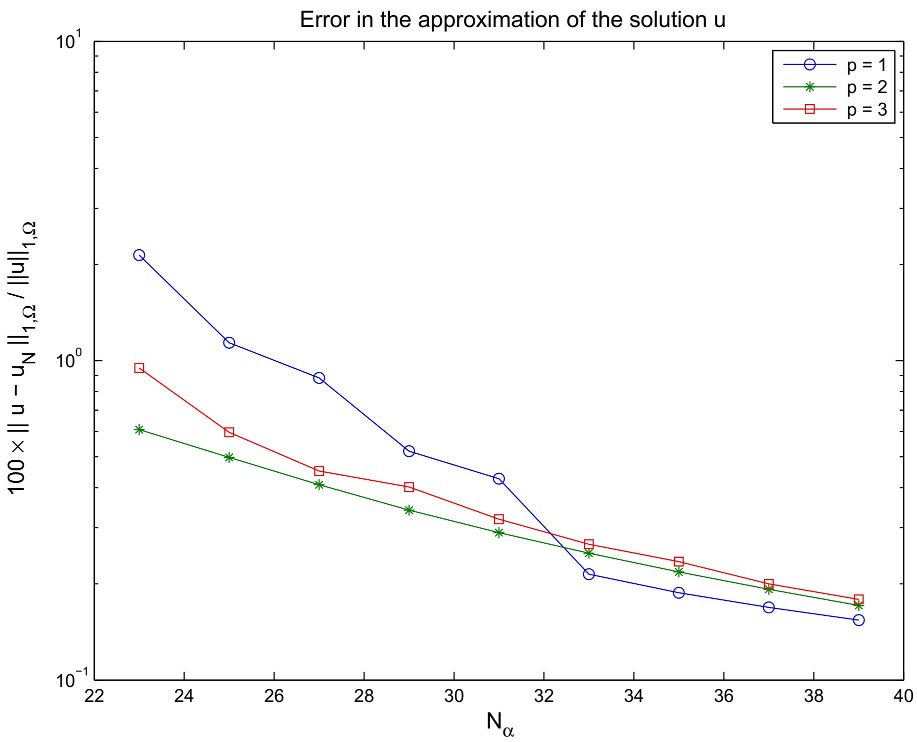

Fig. 9. Convergence of the approximate solution u_N, $\alpha = 2$.

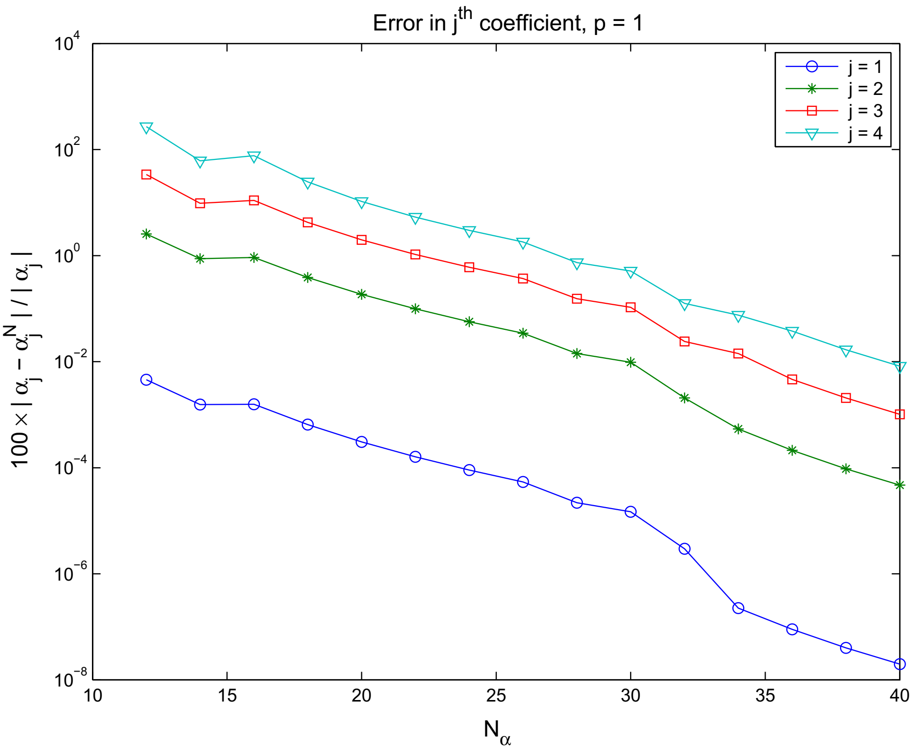

Fig. 10. Convergence of the singular coefficients α_j^N for $p = 1$, $\alpha = 2$.

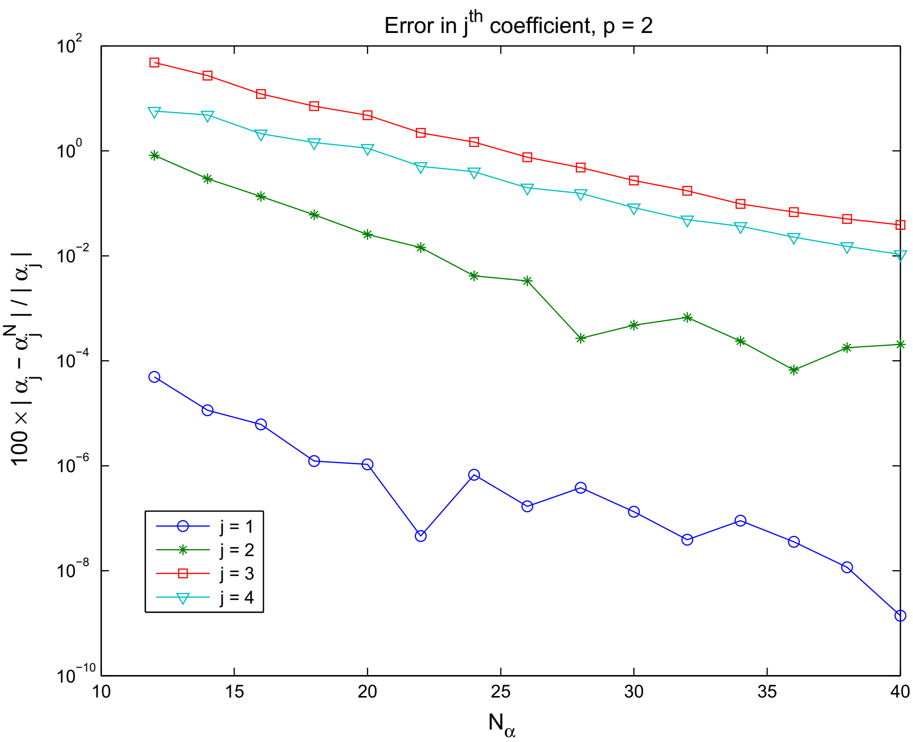

Fig. 11. Convergence of the singular coefficients α_j^N for $p = 2$, $\alpha = 2$.

4.3. L-shaped domain ($\alpha = 1.5$)

Similar results have been obtained with $\alpha = 1.5$, which corresponds to an L-shaped domain. The constant β in (19) was determined as 0.9 from the pair $N_\alpha = 33$, $N_\lambda = 15$. Fig. 13 demonstrates the convergence of the approximate solution, while Figs. 14 and 15 show the convergence of the approximate coefficients (for $p = 1$) and of the Lagrange multipliers, respectively.

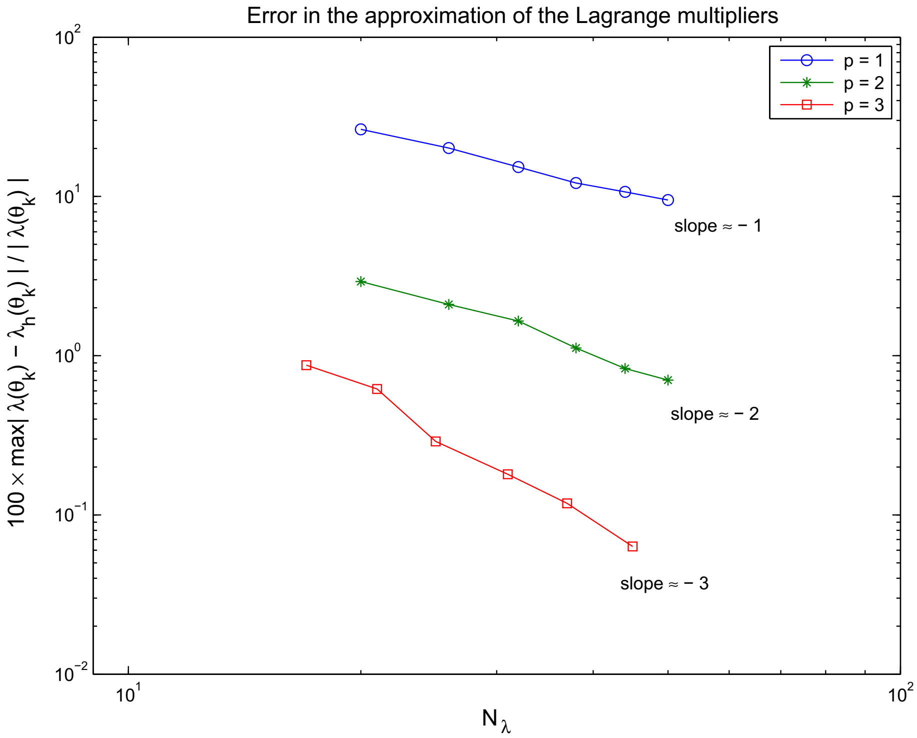

Fig. 12. Convergence of the Lagrange multipliers, $\alpha = 2$.

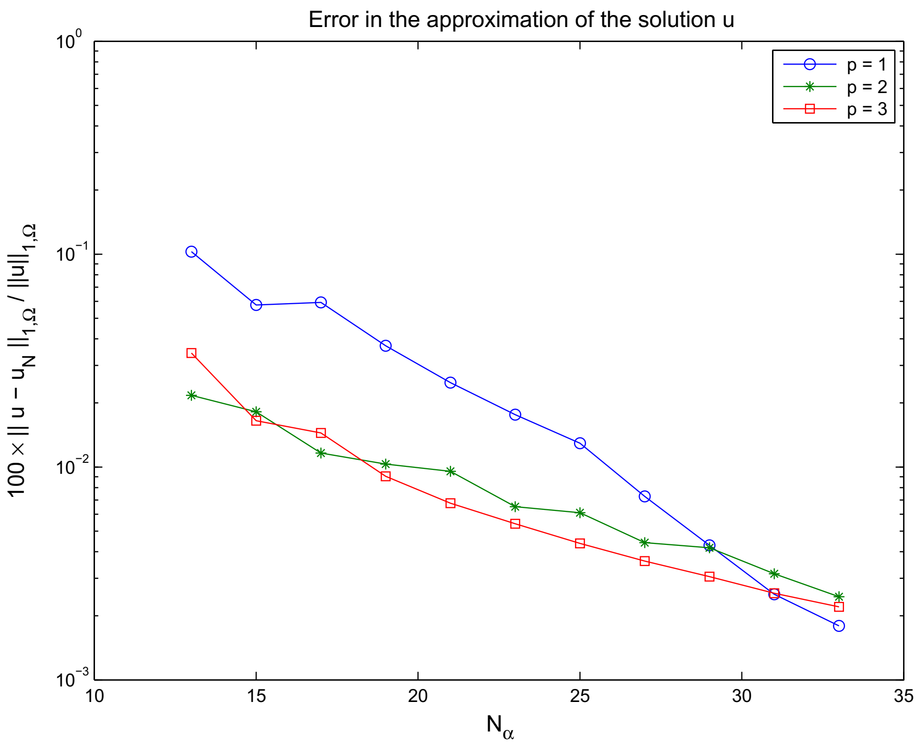

Fig. 13. Convergence of the approximate solution u_N, $\alpha = 1.5$.

5. Conclusions

In this work we revisited the Singular Function Boundary Integral Method (SFBIM) for the solution of two-dimensional elliptic problems with boundary singularities. Our objective was to demonstrate, via numerical examples, the convergence of the method and to show the agreement with the theoretical results provided in the literature. For this purpose the method

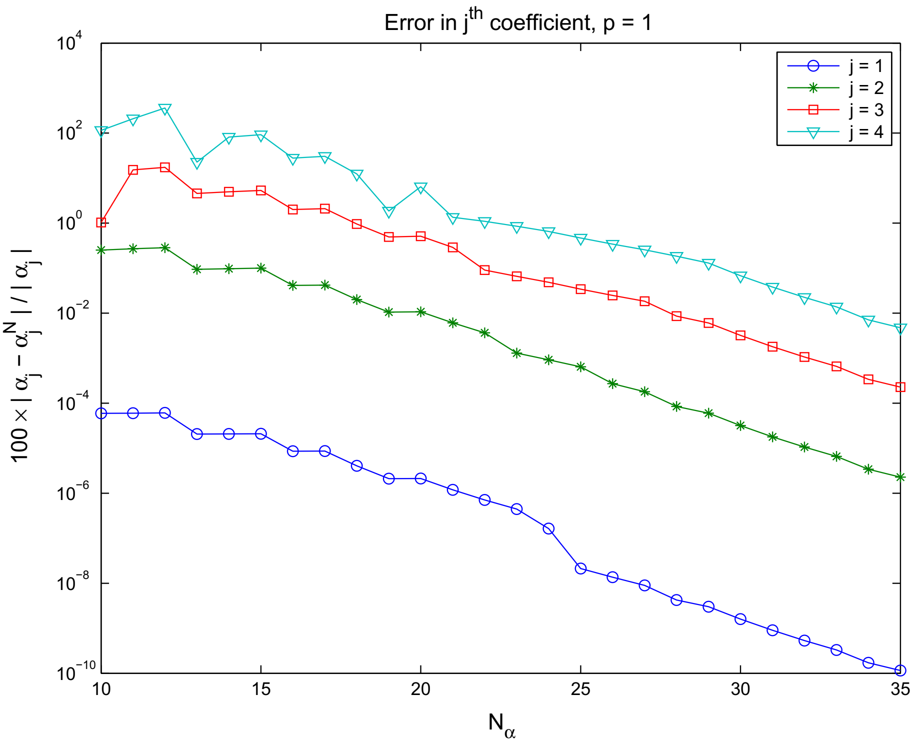

Fig. 14. Convergence of the singular coefficients α_j^N for $p = 1$, $\alpha = 1.5$.

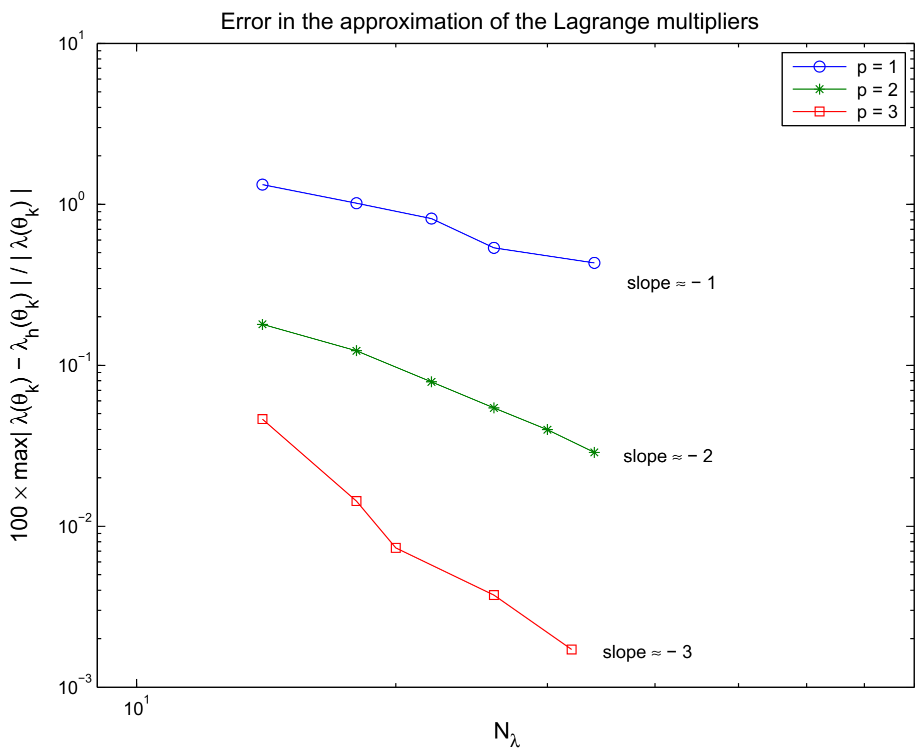

Fig. 15. Convergence of the Lagrange multipliers, $\alpha = 1.5$.

was applied to a Laplacian test problem over a circular sector with the use of constant, linear, quadratic and cubic approximations of the Lagrange multipliers. After obtaining the "optimal" values for the number of Lagrange multipliers and the number of singular functions, the exact approximation errors were calculated. In the cases of linear, quadratic and cubic approximations we show that both the singular coefficients and the solution converge exponentially with the number of singular functions and that the convergence of the approximation of the Lagrange multipliers is algebraic of order p with the number of Lagrange multipliers, as predicted by the theory. In the case of constant approximations, which is not covered by the theory, we observed that the convergence is algebraic for both the singular coefficients and the solution.

Appendix A

In what follows, the elements of the matrix K and the vector F defined in (17) and (18) are given for the constant, linear, quadratic and cubic approximations of the Lagrange multiplier function λ defined in (12). We note that N is the number of elements:

$$N = \begin{cases} N_\lambda, & p = 0, \\ \frac{N_\lambda - 1}{p}, & p \geqslant 1. \end{cases} \tag{A.1}$$

Constant basis functions:

For constant basis functions we have for $i = 1,2,\ldots,N_\alpha$, $j = 1,2,\ldots,N_\lambda$,

$$K_{ij} = \frac{4R^{\mu_i+1}}{(2i-1)} \sin\frac{(2i-1)(2j-1)\pi}{4N} \sin\frac{(2i-1)\pi}{4N}, \tag{A.2}$$

and for $i = 1,2,\ldots,N_\lambda$,

$$F_i = \frac{R\alpha^2\pi^2}{2N^2}\left[2i - 1 - \frac{3i^2 - 3i + 1}{3N}\right]. \tag{A.3}$$

Linear basis functions:

For linear basis functions we have, for $i = 1,2,\ldots,N_\alpha$,

$$K_{i,1} = \frac{2\alpha R^{\mu_i+1}}{(2i-1)}\left[1 - \frac{2N}{(2i-1)\pi}\sin\frac{(2i-1)\pi}{2N}\right], \tag{A.4}$$

$$K_{i,N_\lambda} = \frac{8\alpha N R^{\mu_i+1}}{\pi(2i-1)^2}\sin\frac{(2i-1)\pi}{4N}\cos\frac{(2i-1)(2N-1)\pi}{4N}, \tag{A.5}$$

and for $i = 1,2,\ldots,N_\alpha$, $j = 2,\ldots,N_\lambda - 1$,

$$K_{ij} = \frac{16\alpha N R^{\mu_i+1}}{\pi(2i-1)^2}\sin^2\frac{(2i-1)\pi}{4N}\sin\frac{(2i-1)(j-1)\pi}{2N}. \tag{A.6}$$

Similarly,

$$F_1 = \frac{R\alpha^2\pi^2}{6N^2}\left(1 - \frac{1}{4N}\right), \tag{A.7}$$

$$F_{N_\lambda} = \frac{R\alpha^2\pi^2}{24N^3}\left(6N^2 - 1\right), \tag{A.8}$$

and for $j = 2,\ldots,N_\lambda - 1$,

$$F_i = -\frac{R\left(12N(1-i) + 6i^2 - 12i + 7\right)}{12N^3}. \tag{A.9}$$

Quadratic basis functions:

For quadratic basis functions we have for $i = 1,2,\ldots,N_\alpha$,

$$K_{i,1} = \frac{R^{\mu_i+1}}{2h^2\mu_i^3}\left\{2\cos\left(2h\mu_i\right) + h\mu_i\sin\left(2h\mu_i\right) - 2 + 2h^2\mu_i^2\right\}, \tag{A.10}$$

$$K_{i,2N+1} = -\frac{R^{\mu_i+1}}{2h^2\mu_i^3}\left[-3h\mu_i\sin(2hN\mu_i) + (2h^2\mu_i^2 - 2)\cos(2hN\mu_i) + 2\cos(2h(N-1)\mu_i) - h\mu_i\sin(2h(N-1)\mu_i)\right], \tag{A.11}$$

$$K_{i,2k} = -\frac{2R^{\mu_i+1}}{h^2\mu_i^3}\left[\cos(2hk\mu_i) + h\mu_i\sin(2hk\mu_i) - \cos(2h(k-1)\mu_i) + h\mu_i\sin(2h(k-1)\mu_i)\right], \quad k = 1,\ldots,N, \tag{A.12}$$

$$K_{i,2k+1} = -\frac{R^{\mu_i+1}}{2h^2\mu_i^3}\left[-6h\mu_i\sin(2hkk\mu_i) - 2\cos(2h(k+1)\mu_i) + 2\cos(2h(k-1)\mu_i) - h\mu_i\sin(2h(k+1)\mu_i) - h\mu_i\right],$$
$$k = 1,\ldots,N-1, \tag{A.13}$$

Similarly,

$$F_1 = \frac{R\alpha^2\pi^2}{120N^3}, \tag{A.14}$$

$$F_{2k} = \frac{R\alpha^2\pi^2}{30N^3}[10k(k-1)+10N(1-2k)+3], \quad k=2,3,\ldots,N, \tag{A.15}$$

$$F_{2k+1} = \frac{R\alpha^2\pi^2}{60N^3}\left[10k^2-20kN-1\right], \quad k=1,2,\ldots,N-1, \tag{A.16}$$

$$F_{2N+1} = \frac{R\alpha^2\pi^2}{120N^3}\left[10N^2+1\right]. \tag{A.17}$$

Cubic basis functions:
For cubic basis functions we have for $i = 1,2,\ldots,N_\alpha$,

$$K_{i,1} = -\frac{R^{\mu_i+1}}{3h^3\mu_i^4}\left[(\mu_i^2h^2-3)\sin(3h\mu_i)+3\mu_i h\cos(3h\mu_i)+6h\mu_i-3h^3\mu_i^3\right], \tag{A.18}$$

$$K_{i,3k+2} = -\frac{R^{\mu_i+1}}{2h^3\mu_i^4}\left[-8h\mu_i\cos(3h(k+1)\mu_i)+(6-3h^2\mu_i^2)\sin(3h(k+1)\mu_i)-10h\mu_i\cos(3hk\mu_i)+(6h^2\mu_i^2-6)\sin(3hk\mu_i)\right],$$
$$k=0,1,\ldots,N-1, \tag{A.19}$$

$$K_{i,3k+3} = \frac{R^{\mu_i+1}}{2h^3\mu_i^4}\left[-10h\mu_i\cos(3h(k+1)\mu_i)+(6-6h^2\mu_i^2)\sin(3h(k+1)\mu_i)-8h\mu_i\cos(3hk\mu_i)+(3h^2\mu_i^2-6)\sin(3hk\mu_i)\right],$$
$$k=0,1,\ldots,N-1, \tag{A.20}$$

$$K_{i,3k+4} = \frac{R^{\mu_i+1}}{3h^3\mu_i^4}\left[(11h^2\mu_i^2-6)\sin(3h(k+1)\mu_i)+(3-h^2\mu_i^2)\sin(3hk\mu_i)-3h\mu_i\cos(3hk\mu_i)-3h\mu_i\cos(3h(k+2)\mu_i)+(3-h^2\mu_i^2)\sin(3h(k+2)\mu_i)\right],$$
$$k=0,1,\ldots,N-2, \tag{A.21}$$

$$K_{i,3N+1} = \frac{R^{\mu_i+1}}{6h^3\mu_i^4}\left[(12h\mu_i-6h^3\mu_i^3)\cos(3hN\mu_i)+(11h^2\mu_i^2-6)\sin(3hN\mu_i)+6h\mu_i\cos(3h(N-1)\mu_i)+(6-2h^2\mu_i^2)\sin(3h(N-1)\mu_i)\right]. \tag{A.22}$$

Similarly,

$$F_1 = \frac{R\alpha^2\pi^2}{240N^3}(4N-1), \tag{A.23}$$

$$F_{3k+2} = \frac{3R\alpha^2\pi^2}{80N^3}(10kN-5k^2+2N-2k), \quad k=0,1,\ldots,N-1, \tag{A.24}$$

$$F_{3k+3} = \frac{3R\alpha^2\pi^2}{80N^3}(8N-8k-3+10kN-5k^2), \quad k=0,1,\ldots,N-1, \tag{A.25}$$

$$F_{3k+4} = \frac{R\alpha^2\pi^2}{120N^3}(30N-30k+30kN-15k^2-16), \quad k=0,1,\ldots,N-2, \tag{A.26}$$

$$F_{3N+1} = \frac{R\alpha^2\pi^2}{240N^3}(15N^2-1). \tag{A.27}$$

References

[1] B. Szabó, I. Babuška, Finite Element Analysis, John Wiley & Sons, New York, 1991.
[2] N. Arad, Z. Yosibash, G. Ben-Dor, A. Yakhot, Comparing the flux intensity factors by a boundary element method for elliptic equations with singularities, Commun. Numer. Meth. Eng. 14 (1998) 657–670.
[3] G. Georgiou, L.G. Olson, Y.S. Smyrlis, A singular function boundary integral method for the Laplace equation, Commun. Numer. Meth. Eng. 12 (1996) 127–134.
[4] M. Elliotis, G. Georgiou, C. Xenophontos, The solution of a Laplacian problem over an L-shaped domain with a singular function boundary integral method, Commun. Numer. Meth. Eng. 18 (2002) 213–222.

[5] C. Xenophontos, M. Elliotis, G. Georgiou, The singular function boundary integral method for elliptic problems with singularities, SIAM J. Sci. Comput. 28 (2006) 517–532.
[6] M. Elliotis, G. Georgiou, C. Xenophontos, The singular function boundary integral method for biharmonic problems with crack singularities, Eng. Anal. Bound. Elem. 31 (2007) 209–215.
[7] Z.C. Li, T.T. Lu, H.T. Huang, A. Cheng, Trefftz, collocation, and other boundary methods – A comparison, Numer. Meth. PDEs 23 (2007) 93–144.
[8] F. Bernal, G. Gutierrez, M. Kindelan, Use of singularity capturing functions in the solution of problems with discontinuous boundary conditions, Eng. Anal. Bound. Elem. 33 (2009) 200–208.
[9] A.A. Dosiyev, S.C. Buranay, On solving the cracked-beam problem by block method, Commun. Numer. Meth. Eng. 24 (2008) 1277–1289.